

Photon Beam Diagnostics for VISA FEL

A. Murokh, C. Pellegrini, J. Rosenzweig, P. Frigola, P. Musumeci, A. Tremaine, M. Babzien, I. Ben-Zvi, A. Doyuran, E. Johnson, J. Skaritka, X.J. Wang, K.A. Van Bibber, J.M. Hill, G.P. Le Sage, D. Nguyen, M. Cornacchia

This article was submitted to
1999 Particle Accelerator Conference, New York, NY, March 27-
April 2, 1999

November 5, 1999

U.S. Department of Energy

Lawrence
Livermore
National
Laboratory

DISCLAIMER

This document was prepared as an account of work sponsored by an agency of the United States Government. Neither the United States Government nor the University of California nor any of their employees, makes any warranty, express or implied, or assumes any legal liability or responsibility for the accuracy, completeness, or usefulness of any information, apparatus, product, or process disclosed, or represents that its use would not infringe privately owned rights. Reference herein to any specific commercial product, process, or service by trade name, trademark, manufacturer, or otherwise, does not necessarily constitute or imply its endorsement, recommendation, or favoring by the United States Government or the University of California. The views and opinions of authors expressed herein do not necessarily state or reflect those of the United States Government or the University of California, and shall not be used for advertising or product endorsement purposes.

PHOTON BEAM DIAGNOSTICS FOR VISA FEL

A. Murokh*, C. Pellegrini, J. Rosenzweig, P. Frigola, P. Musumeci, A. Tremaine, UCLA
 M. Babzien, I. Ben-Zvi, A. Doyuran, E. Johnson, J. Skaritka, X. J. Wang, BNL
 K. A. Van Bibber, J. M. Hill, G. P. Le Sage, LLNL
 D. Nguyen, LANL
 M. Cornacchia, SLAC

Abstract

The VISA (Visible to Infrared SASE Amplifier) project is designed to be a SASE-FEL driven to saturation in the sub-micron wavelength region. Its goal is to test various aspects of the existing theory of Self-Amplified Spontaneous Emission, as well as numerical codes. Measurements include: angular and spectral distribution of the FEL light at the exit and inside of the undulator; electron beam micro-bunching using CTR; single-shot time resolved measurements of the pulse profile, using auto-correlation technique and FROG algorithm. The diagnostics are designed to provide maximum information on the physics of the SASE-FEL process, to ensure a close comparison of the experimental results with theory and simulations.

1 INTRODUCTION

The concept of self-amplified spontaneous emission [1] free electron lasers is of the great interest from both academic and practical point of view. The description of the process is a complicated relativistic theory on the merger of accelerator physics, radiation theory and plasma physics. The technological prospects are very promising, as it allows, among other things, the construction of the x-ray laser [2]. However, the experimental proof of SASE-FEL theory has taken place at much larger wavelengths (e.g. UCLA-LANL experiment in IR [3]). The objective for this device is to scale the experimental confirmation of theory and simulation into the visible and near IR region, as well as measure saturation and other different aspects of FEL performance.

The experiment will be held at the Accelerator Test Facility in Brookhaven National Laboratory [4]. It is a state of the art photoinjector accelerator, which can provide an electron beam of the desired quality (Table 1).

The undulator consists of four 1-meter long sections. It utilizes an array of focusing magnets, to provide a strong focusing in both planes, in order to minimize the bunch spot size. Optimization of the electron trajectories in the undulator is being done with the pulsed wire correction technique [5]. In addition, the external trim coils are built to minimize the trajectory walk-off during operation.

2 MEASUREMENTS

Achieving the maximum gain in the first harmonic, is a proof of principle experiment, to demonstrate the operation of SASE-FEL at shorter wavelengths.

Table 1: Relevant parameters for VISA FEL

Nominal Beam Energy	71MeV
Peak Current	200 Amp
Charge	1nC
Normalized Beam Emittance	2π -mm-mrad
Undulator Parameter, K	1.26
Undulator Period	1.8 cm
Number of Periods, N_U	220
Electron Beam Beta-Function	30 cm
Radiation Wavelength, λ_r	800nm

The single particle spontaneous emission intensity within the coherent angle [6], for the VISA undulator is 1.5 photons per 100 electrons, which corresponds, in case of 200A beam, to the total radiated power of

$$P_{SE} = .52 \frac{ek_r I_p}{\pi \epsilon_0} = 4.7W \quad (1)$$

In order to saturate starting from noise, the FEL process has to proceed through at least 10 field gain lengths. The design parameters are chosen such that it is just enough to saturate over the length of 4 meters. For the 1nC beam the saturated power, according to simulations, is 60MW, which attributes to the total gain of $G=1.3 \cdot 10^7$.

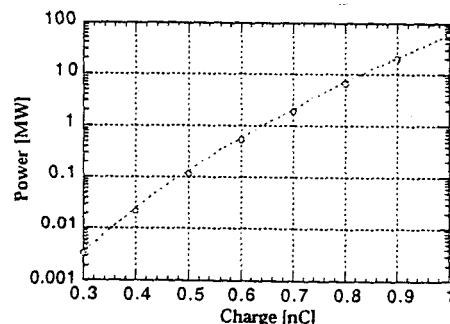


Figure 1: FEL radiation power dependence on charge

* alex@stout.physics.ucla.edu

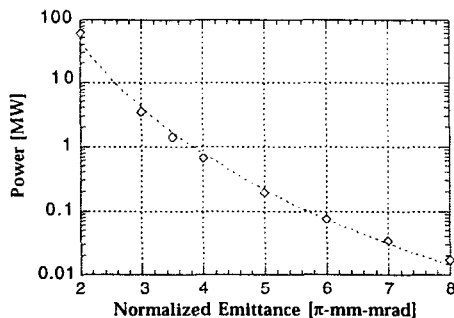


Figure 2: FEL power degradation due to the electron beam emittance increase

2.1 Power versus Charge

The measurement can be repeated for different charges, which should give a characteristic exponential curve on Fig. 1. However, the actual performance of the FEL will depend on the experimental conditions, such as quality of the beam, undulator performance, and proper matching and guiding of the beam through the undulator. Particularly important is the emittance of the beam. On Fig.2 there are simulations results for 1nC beam with the peak current of 200A, which demonstrate very rigid requirements to meet the designed performance of the FEL. Increase in the average beam size by 20% would lower the radiation power by a factor of 4. To ensure proper control of the beam spot, the vacuum chamber is equipped with a YAG beam profile monitors every 50cm.

2.2 Spectral and Angular Fluence

After the exit of the undulator, the light will be transported into the measurements area, attenuated if necessary and then processed by the diagnostics. Relay imaging will be used to preserve profile and characteristics of a radiation pulse, during the transport.

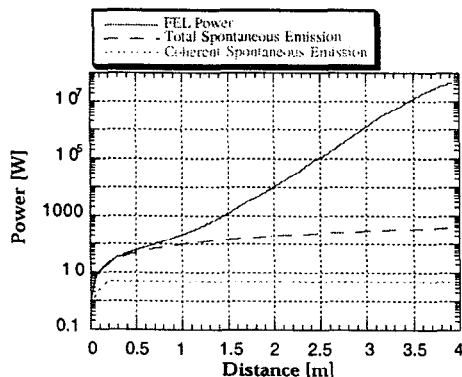


Figure 3: Simulations results for the radiation power along the length of the undulator

For the direct comparison of experimental results with the theory of SASE-FEL process, not only the radiation intensity, but also its spectral and angular distribution in the far field will be measured.

Expanding, and collimating the beam into the CCD array shall provide an accurate measurement of the total angular fluence; whereas the slit spectrometer will enable to obtain explicit results for $dI^2/d\omega d\Omega$.

2.3 Power Gain along the Undulator

VISA FEL design makes possible a set of rather novel measurements. First of all, it is a power gain along the undulator length. Fig. 3 shows the simulations of the power growth along the VISA undulator, performed with the GENESIS code. It indicates nearly linear behavior along at the beginning of the undulator (lethargy), where radiation is being dominated by the spontaneous emission (dashed line). The coherent fraction of SE (dotted line) starts the FEL process, and in a few gain lengths the exponential term prevails, providing for the overall high gain.

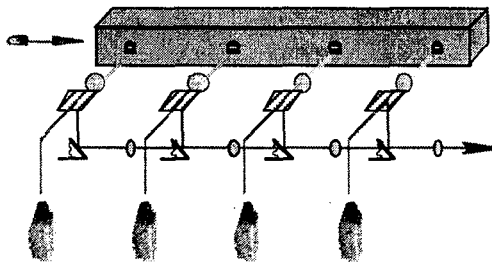


Figure 4: Optical diagnostics layout. Coated mirrors separate FEL radiation from the YAG light and send it into the relay imaging transport line.

In order to make that measurement possible, the undulator chamber was equipped with 8 diagnostics ports, 50cm apart. The probes are set up with both, YAG crystals for the electron beam diagnostics, and mirrors to get the FEL radiation out. Probe design utilizes periscope mirrors to compensate for mechanical hysteresis in the actuators. The optical transport system has been designed to provide for the optimal imaging of the FEL radiation into the diagnostics area. To satisfy the requirements of the experiment, the transport system should:

- provide for minimum losses, transporting the FEL radiation beam over 15-20 m;
- ensure the identical imaging properties for all ports;
- tolerate errors and imperfections in the optics.

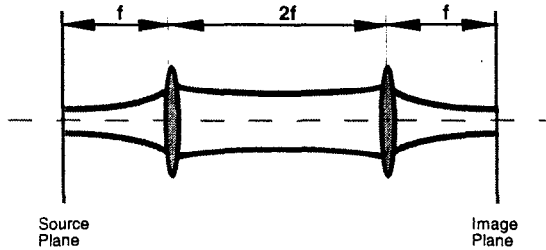


Figure 5: Single cell of the optical transport system

The design satisfying for these demands, is shown on Fig. 4. The light from the probe comes out through the vacuum window where it is being split by the mirror coated for 800nm. Most of the YAG light travels through the mirror into the camera, whereas FEL radiation gets into the transport line via the flipping mirror, which is automated to move in and out of the light path, so that it would not interfere with the light from a previous port.

In the transport line, the radiation light will go through the periodic lens array, converging to the identical image after each cell, shown on Fig. 5. It is straightforward, that this configuration translates the image into its identity, rotated 180°:

$$M = \begin{pmatrix} 1 & f \\ 0 & 1 \end{pmatrix} \begin{pmatrix} 1 & 2f \\ -\frac{1}{f} & -1 \end{pmatrix} \begin{pmatrix} 1 & f \\ -\frac{1}{f} & 0 \end{pmatrix} = \begin{pmatrix} -1 & 0 \\ 0 & -1 \end{pmatrix} \quad (2)$$

Since the diagnostics ports are separated by 50 cm, we found the choice of 25-cm focal lengths to be the most adequate. One can see on Fig. 4, that with the proper positioning of lenses, the transport for each port will contain a series of 1 to 4 unit cells, before the common image plane. From there, the similar but more spread-out system will provide a long-range transport.

Such a transport system provides a unit magnification imaging from all the ports, with insignificant diffraction losses for the number of Hermit-Gaussian modes, including the fundamental. Another important advantage is, that it leaves no space for the systematic errors, so the

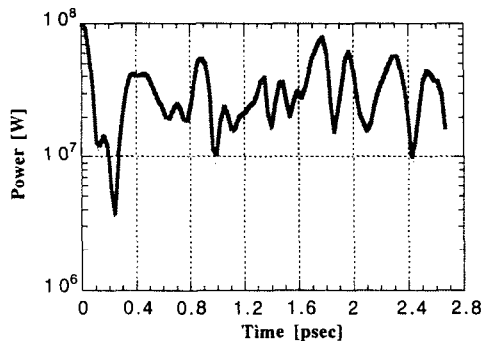


Figure 6: Spikes in the radiation temporal profile (Average period is 94 psec)

tolerance is fairly high. The 5-cell array preserves all properties of the Gaussian beam within 95%, while the lens positioning accuracy is 0.5cm, focal length - 0.5%, and angular mismatch at injection - 10mrad.

3 TIME DOMAIN DIAGNOSTICS

Spikes formation is another important property of SASE-FEL process. For VISA beam, the bunch length exceeds the cooperation length by two orders of magnitude, so the multiple spikes formation is anticipated [7] with the period of not bigger than 100 psec. The time structure of the radiation pulse is shown on Fig. 6. Presence of spikes can be established indirectly, by measuring the radiation spectrum and power fluctuations [7] at the undulator exit, as it was done in previous experiment [3].

For the direct measurement of the radiation beam temporal profile the single shot autocorrelator was developed at LLNL specifically for 800nm light. By utilizing a thinner crystal and narrowing the bandwidth it allows resolving a femtosecond structures in a pulse. With that tool the FEL radiation can be characterized completely, using the FROG algorithm.

4 CTR MICROBUNCHING MONITOR

Bunching of an electron beam (b_i) in the undulator can be measured directly by sending a bunched beam through a thin foil, and observing a backscattered coherent transition radiation [8]. The FEL radiation transport line and diagnostics can be used to propagate and characterize the CTR signal, respectively. Total intensity of the CTR at FEL wavelength is directly proportional to b_i^2 .

The results of a similar measurement in UCLA-LANL experiment [9] were in an excellent agreement with the FEL data. It was a little surprising, that the spectrum of the CTR signal was ~3% off, compare to the FEL radiation. One can speculate that the difference can be attributed to the sidebands in the SASE radiation, due to spikes. However, another experimental verification is necessary to fully understand the phenomenon.

5 REFERENCES

- [1] R. Bonifacio, C. Pellegrini, and L. Narducci, Opt. Commun. **50**, 313 (1984)
- [2] "Linac Coherent Light Source (LCLS) Design Study Report", The LCLS Design Study Group, SLAC Report No. SLAC-R-521 (1998)
- [3] M. Hogan *et al.*, "Measurements of Gain Larger than 10^5 at 12 μm in a Self-Amplified Spontaneous-Emission Free-Electron Laser", Phys. Rev. Lett. **81**, 4867 (1998)
- [4] D. Palmer *et al.*, AIP Conference Proceedings **398**, 695 (1997)
- [5] R.W. Warren, Nucl. Instrum. Methods Phys. Res., Sect. A, **272**, 257 (1988)
- [6] J.B. Murphy, C. Pellegrini, "Introduction to the Physics of Free-Electron Laser", Laser Handbook, **6** (1990)
- [7] R. Bonifacio *et al.*, Phys. Rev. Lett. **73**, 70 (1994)
- [8] J.B. Rosenzweig, G. Travish, and A. Tremaine, Nucl. Instrum. Methods Phys. Res., Sect. A **365**, 255 (1995)
- [9] A. Tremaine *et al.*, Phys. Rev. Lett. **81**, 5816 (1998)

This work was performed at the University of California, Lawrence Livermore National Laboratory, under the auspices of the U.S. Department of Energy (Contract #W-7405-Eng.-48).